Reactions of Low-Valent Group V Dicarbonyl Phosphine Complexes with Carbon-Based Electrophiles To Produce Metal Alkyl, Acyl, Carbyne, and Acetylene Complexes

Brian S. Bronk, John D. Protasiewicz, Laura E. Pence, and Stephen J. Lippard*

Department of Chemistry, Massachusetts Institute of Technology, Cambridge, Massachusetts 02139

Received December 22, 1994[⊗]

The $[V(CO)_2(dmpe)_2]^-$ anion reacts with Et_3OBF_4 and EtOTf to afford the unexpected product of formal C-alkylation, $[V(\eta^2\text{-}C(O)Et)(CO)(dmpe)_2]$, which has been structurally characterized by X-ray crystallography (space group $Pna2_1$, a = 12.917(2) Å, b = 12.335(2) Å, c = 14.331(2) Å, V = 2283.4(5) Å^3). The formation of species derived by O-acylation of the CO ligands in the $[Ta(CO)_2(dmpe)_2]^-$ and $[Ta(CO)_2(depe)_2]^-$ anions was indirectly established by isolation and characterization of products in which two CO ligands had coupled to form acetylene complexes. Addition of 2 equiv of acetyl chloride to $Na[Ta(CO)_2(dmpe)_2]$ or $Na[Ta(CO)_2(depe)_2]$ yielded the acetylene complexes [Ta(AcOC≡COAc)(dmpe or depe)$_2$Cl]. The structure of the dmpe derivative was confirmed in a single-crystal X-ray determination (space group $C2$, a = 14.964(2) Å, b = 11.960(2) Å, c = 31.710(5) Å, β = 102.77(1)°, V = 5535(1) Å^3). Additional proof of direct alkylation at terminal CO ligands was provided by isolation of mixed siloxy/alkoxyacetylene coupled products $[M(R'_3SiOC{\equiv}COR)(dmpe)_2X]$ (R = Et, Ac, CO_2Me; R'_3Si = ^{t}BuPh$_2$Si, ^{i}Pr$_3$Si) and $[M(R'_3SiOC{\equiv}COR)(depe)_2X]$ (R = Et, Ac; R'_3Si = ^{t}BuPh$_2$Si, ^{i}Pr$_3$Si, Me$_3$Si) from reactions of the siloxycarbyne precursors $[M(COSiR'_3)(CO)(dmpe)_2]$ and $[M(COSiR'_3)(CO)(depe)_2]$ (M = Nb, Ta) with carbon-based electrophiles. The proper choice of carbon-based electrophile and reaction conditions is crucial in order to avoid oxidation of these low-valent metal complexes to $[M(CO)_2(dmpe)_2X]$, which can occur competitively or exclusively.

Introduction

The reductive coupling of two carbon monoxide ligands in $[M(CO)_2(Me_2PCH_2CH_2PMe_2)_2X]$ complexes occurs according to the mechanism outlined in Scheme 1.[1] This transformation was originally discovered[2] following studies of reductive coupling in related isocyanide complexes[3,4] and has since been applied by us and others in the synthesis of a wide variety of related metal acetylene complexes.[2,5–21] As indicated in the scheme,

Scheme 1

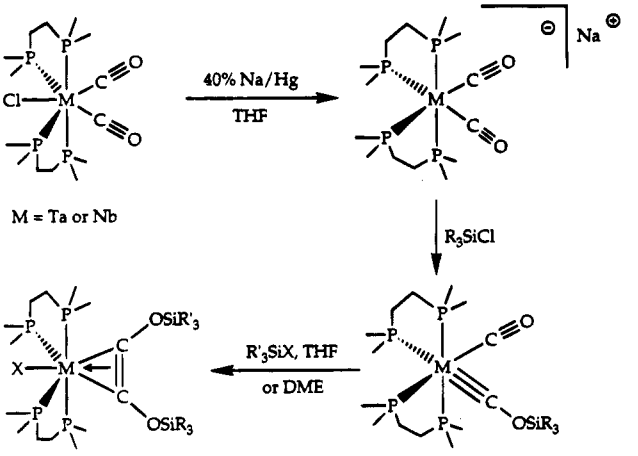

the reaction proceeds by electrophilic attack of a silyl reagent on the carbonyl oxygen atoms of the highly reduced dicarbonyl anion in two sequential steps. The first step leads to a siloxycarbyne and the second to the coupled product. This mechanism differs from that commonly encountered in the coupling of carbyne and CO ligands in many other systems, which often involves

⊗ Abstract published in *Advance ACS Abstracts,* April 1, 1995.

(1) Carnahan, E. M.; Protasiewicz, J. D.; Lippard, S. J. *Acc. Chem. Res.* **1993**, *26*, 90.
(2) Bianconi, P. A.; Williams, I. D.; Engeler, M. P.; Lippard, S. J. *J. Am. Chem. Soc.* **1986**, *108*, 311.
(3) Lam, C. T.; Corfield, P. W. R.; Lippard, S. J. *J. Am. Chem. Soc.* **1977**, *99*, 617.
(4) Lam, C. T.; Novotny, M.; Lewis, D. L.; Lippard, S. J. *Inorg. Chem.* **1978**, *17*, 2127.
(5) Vrtis, R. N.; Liu, S.; Rao, C. P.; Bott, S. G.; Lippard, S. J. *Organometallics* **1991**, *10*, 275.
(6) Acho, J. A.; Lippard, S. J. *Organometallics* **1994**, *13*, 1294.
(7) Bianconi, P. A.; Vrtis, R. N.; Rao, C. P.; Williams, I. D.; Engeler, M. P.; Lippard, S. J. *Organometallics* **1987**, *6*, 1968.
(8) Bronk, B. S.; Protasiewicz, J. D.; Lippard, S. J. *Organometallics* **1995**, *14*, 1385.
(9) Carnahan, E. M.; Lippard, S. J. *J. Am. Chem. Soc.* **1990**, *112*, 3230.
(10) Carnahan, E. M.; Lippard, S. J. *J. Chem. Soc., Dalton Trans.* **1991**, 699.
(11) Carnahan, E. M.; Lippard, S. J. *J. Am. Chem. Soc.* **1992**, *114*, 4166.
(12) Protasiewicz, J. D.; Lippard, S. J. *J. Am. Chem. Soc.* **1991**, *113*, 6564.
(13) Protasiewicz, J. D.; Bronk, B. S.; Masschelein, A.; Lippard, S. J. *Organometallics* **1994**, *13*, 1300.
(14) Vrtis, R. N.; Lippard, S. J. *Isr. J. Chem.* **1990**, *30*, 331.
(15) Warner, S.; Lippard, S. J. *Organometallics* **1986**, *5*, 1716.
(16) Filippou, A. C.; Grünleitner, W. *J. Organomet. Chem.* **1990**, *393*, C10.
(17) Filippou, A. C.; Grünleitner, W. *Z. Naturforsch.* **1991**, *46B*, 216.
(18) Filippou, A. C.; Grünleitner, W.; Völkl, C.; Kiprof, P. *Angew. Chem., Int. Ed. Engl.* **1991**, *30*, 1167.
(19) Filippou, A. C.; Völkl, C.; Grünleitner, W.; Kiprof, P. *J. Organomet. Chem.* **1992**, *434*, 201.
(20) Pombeiro, A. J. L.; Richards, R. L. *Coord. Chem. Rev.* **1990**, *104*, 13.
(21) Fraústo da Silva, J. J. R.; Pellinghelli, M. A.; Pombeiro, A. J. L.; Richards, R. L.; Tiripicchio, A.; Wang, Y. *J. Organomet. Chem.* **1993**, *454*, C8.

0276-7333/95/2314-2177$09.00/0

Scheme 2

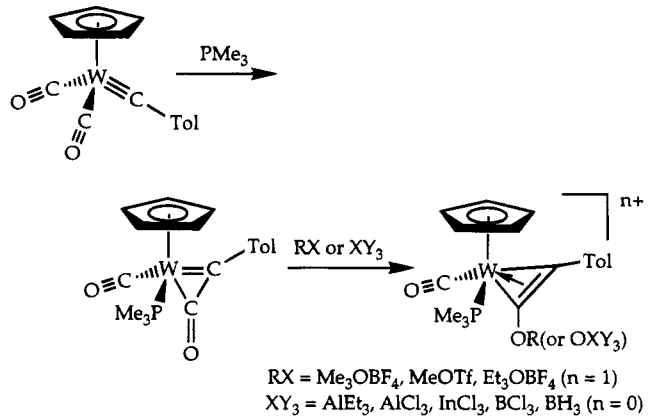

an η^2-ketenyl intermediate, as illustrated for one case in Scheme 2.[22,23] A metal-bound ketenyl oxygen atom is significantly more activated toward electrophilic attack compared even to the electron-rich carbonyl complexes used in the reductive coupling reaction of Scheme 1. A detailed kinetic analysis clearly indicated, however, that the first step in converting the siloxycarbyne to the coupled product was silylation of the adjacent CO ligand, and no evidence was found to indicate the participation of an η^2-ketenyl species.[13,24]

One conspicuous facet of the CO-coupling chemistry in Scheme 1 is the fact that, up to the present, silyl-based electrophiles have been required. Reactions of carbon-based electrophiles with complexes containing terminal CO ligands usually occur at the metal center.[25] Previous work established that treatment of Na[Ta(CO)$_2$(dmpe)$_2$] with alkylating reagents affords a tantalum alkyl species (eq 1) rather than the carbyne or

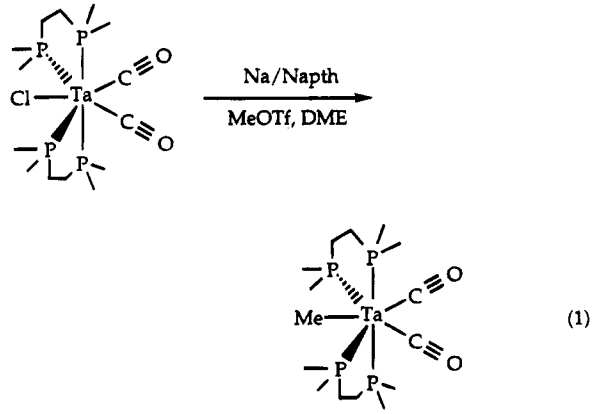

(1)

coupled product.[26] The success of silyl-based electrophiles was attributed to the extra driving force obtained by formation of Si–O bonds, which are considerably stronger than M–Si bonds. This difference might direct electrophilic attack at the oxygen atom of the terminal CO ligand, rather than the metal center. Alternatively, it might be argued that silyl-based reagents are more sterically encumbered than alkylating reagents, hindering formation of a metal–silicon bond. The importance of such steric factors is underscored by reactions of the vanadium compound Na[V(CO)$_2$(dmpe)$_2$] with Me$_3$SiOTf and EtOTf to produce respectively the novel species [V(Me$_3$SiOC≡COSiMe$_3$)(dmpe)$_2$]OTf, communicated previously,[12] and [V(η^2-C(O)Et)(CO)(dmpe)$_2$], described in the present article.

Electrophilic attack at the oxygen atom of metal carbonyl species is most facile for complexes having bridging CO ligands. A variety of electrophiles has been employed,[27] including mineral acids,[28,29] Lewis acids, and alkylating[28,30–33] or acylating reagents.[28] In complexes with terminal CO ligands, the metal center appears to be the preferred site of attack by protic acids, although Lewis acids can exhibit some affinity for the oxygen atom. Reactions of this kind have most frequently been probed with anionic carbonyl complexes and alkylating reagents.[34–37] Attempts to acylate these complexes gave exclusive addition to the metal center.[35,36] Acylation reactions have not received as much attention, however, since acyl complexes can be readily prepared by alkylation at the metal center, followed by alkyl migration to a carbonyl ligand.

In the present work we have achieved the reductive coupling of two CO ligands by using acyl groups as carbon-based electrophiles. This reaction significantly extends the scope of reductively coupled products accessible by the chemistry outlined in Scheme 1. In addition, we have delineated some of the conditions which dictate the site of carbon-based electrophilic attack on low-valent metal carbonyl complexes.

Experimental Section

General Considerations. All reactions and manipulations were carried out either in a Vacuum Atmospheres drybox under a dinitrogen atmosphere or by standard Schlenk techniques under an argon atmosphere. Solutions were stirred magnetically with a Teflon-covered stirbar unless noted otherwise. Solvents (THF, DME, Et$_2$O, and pentane) were distilled under dinitrogen from sodium benzophenone ketyl. Benzene-d_6 was dried by passage through a column of alumina and stored under dinitrogen. Tetramethylsilane was distilled from calcium hydride and stored under dinitrogen. Acetyl chloride and methyl chloroformate were distilled and stored under dinitrogen. All other reagents were used as received after degassing. Proton chemical shifts were referenced to residual solvent peaks. ^{31}P NMR spectra were referenced to external phosphoric acid. ^{1}H, ^{31}P, and ^{13}C NMR spectra were recorded on a Varian XL 300 instrument at 300, 121, and 75.5 MHz, respectively. Infrared (IR) spectra were recorded on a Biorad FTS-7 spectrophotometer. Elemental analyses were performed by Oneida Research Laboratories, Whitesboro, NY.

(22) Kreissl, F. R.; Frank, A.; Schubert, U.; Lindner, T. L.; Huttner, G. *Angew. Chem., Int. Ed. Engl.* **1976**, *15*, 632.
(23) Kreissl, F. R.; Eberl, K.; Uedelhoven, W. *Chem. Ber.* **1977**, *110*, 3782.
(24) Protasiewicz, J. D.; Masschelein, A.; Lippard, S. J. *J. Am. Chem. Soc.* **1993**, *115*, 808.
(25) King, R. B. *Acc. Chem. Res.* **1970**, *3*, 417.
(26) Datta, S.; Wreford, S. S. *Inorg. Chem.* **1977**, *16*, 1134.
(27) Adams, R. D.; Horvath, I. T. *Prog. Inorg. Chem.* **1985**, *33*, 133.
(28) Hodali, H. A.; Shriver, D. F. *Inorg. Chem.* **1979**, *18*, 1236.
(29) Whitmore, K.; Shriver, D. F. *J. Am. Chem. Soc.* **1980**, *102*, 1456.
(30) Shriver, D. F.; Lehman, D.; Strope, D. *J. Am. Chem. Soc.* **1975**, *97*, 1594.
(31) Green, M.; Mead, K. A.; Mills, R. M.; Salter, I. D.; Stone, F. G. A.; Woodward, P. *J. Chem. Soc., Chem. Commun.* **1982**, 51.
(32) Johnson, B. F. G.; Lewis, J.; Orpen, A. G.; Raithby, P. R.; Süss, G. *J. Organomet. Chem.* **1979**, *173*, 187.
(33) Gavens, P. D.; Mays, M. J. *J. Organomet. Chem.* **1978**, *162*, 389.
(34) Gladysz, J. A.; Williams, G. M.; Tam, W.; Johnson, D. L.; Parker, D. W.; Selover, J. C. *Inorg. Chem.* **1979**, *18*, 553.
(35) Heck, R. F.; Breslow, D. S. *J. Am. Chem. Soc.* **1962**, *84*, 2499.
(36) Hieber, W.; Duchatsch, H. *Chem. Ber.* **1965**, *98*, 1744.
(37) Lai, C.-K.; Feighery, W. G.; Zhen, Y.; Atwood, J. D. *Inorg. Chem.* **1989**, *28*, 3929.

$[Ta(CO)_2(dmpe)_2Cl]$,[38] $[Ta(CO)_2(depe)_2Cl]$,[38] $[Nb(CO)_2(dmpe)_2Cl]$,[38] $Na[V(CO)_2(dmpe)_2]$,[12] $[Ta(COSi^tBuPh_2)(CO)(dmpe)_2]$,[13] and $[Ta(COSi^iPr_3)(CO)(dmpe)_2]$[5] were prepared by following literature procedures. $[Ta(^{13}CO)_2(dmpe)_2Cl]$ was prepared with ^{13}CO (99%, Cambridge Isotopes Lab).

$[Ta(EtOC{\equiv}COSi^tBuPh_2)(dmpe)_2OTf]$ (1a). A 25-mL, one-necked, pear-shaped flask fitted with a rubber septum was charged with $[Ta(COSi^tBuPh_2)(CO)(dmpe)_2]$ (0.117 g, 0.15 mmol) and 10 mL of DME. Upon dissolution, EtOTf (0.020 mL, 0.027 g, 0.15 mmol) was added in one portion via syringe. The reaction mixture was stirred for 1.5 h, during which time the color changed from deep red to green-brown. The solvents were removed under vacuum, and the residue was triturated with two 10-mL portions of pentane. The product was extracted with 15 mL of pentane, the extract was filtered, and the solvents were removed under vacuum to provide a green-brown solid. Recrystallization from pentane at −30 °C afforded 0.043 g (30%) of **1a** as a dark green solid. IR (Nujol): 1609, 1318, 1236, 1204, 1166, 1101, 1024, 970, 937, 732, 703 cm^{-1}. ^1H NMR (300 MHz, C_6D_6): δ 7.59−7.63 (m, 4 H), 7.13−7.16 (m, 6 H), 2.76 (q, J = 7.0 Hz, 2 H), 1.83 (bs, 8 H), 1.61 (bs, 12 H), 1.48 (s, 12 H), 1.07 (s, 9 H), 0.29 (t, J = 7.0 Hz, 3 H). ^{31}P NMR (121 MHz, C_6D_6): δ 34.2. Anal. Calcd for $C_{33}H_{56}F_3O_5P_4SSiTa$: C, 41.51; H, 5.91; N, 0.00. Found: C, 41.86; H, 5.84; N, 0.00.

$[Ta(EtOC{\equiv}COSi^iPr_3)(dmpe)_2OTf]$ (1b). A 25-mL, one-necked, pear-shaped flask fitted with a rubber septum was charged with $[Ta(CO)_2(dmpe)_2Cl]$ (0.143 g, 0.25 mmol) and 10 mL of THF. Upon dissolution, excess 40% sodium amalgam was added and the reaction mixture was stirred vigorously for 4 h. The resulting orange solution was decanted into a second 25-mL, one-necked, pear-shaped flask fitted with a rubber septum, and $^iPr_3SiCl$ (0.054 mL, 0.048 g, 0.25 mmol) was added in one portion via syringe, resulting in a dark red solution. After the mixture was stirred for an additional 15 min, the solvents were removed under vacuum, the product was triturated with two 10-mL portions of pentane and extracted with 10 mL of pentane, the extract was filtered, and the solvents were removed under vacuum to provide 0.166 g (0.24 mmol) of a red solid, unpurified $[Ta(COSi^iPr_3)(CO)(dmpe)_2]$. This material was dissolved in 5 mL of DME in a 25-mL, one-necked, pear-shaped flask fitted with a rubber septum, and EtOTf (0.031 mL, 0.043 g, 0.24 mmol) was added in one portion via syringe. The reaction mixture was stirred for 40 min, during which time the color changed from deep red to green-brown. The solvents were removed under vacuum, the product was extracted with 15 mL of pentane, the extract was filtered, and the pentane was removed under vacuum. Crystallization from pentane at −30 °C provided 0.092 g (42% for two steps) of **1b** as green-brown crystals. IR (Nujol): 1606, 1322, 1233, 1202, 1171, 1116, 1018, 971, 942, 928, 884, 722 cm^{-1}. ^1H NMR (300 MHz, C_6D_6): δ 3.75 (bq, 2 H), 1.51−1.86 (m, 20 H), 1.36 (s, 12 H), 1.11−1.25 (m, 3 H), 1.05 (d, J = 7.0 Hz, 18 H), 1.04−1.05 (m, 3H). ^{13}C NMR (75.5 MHz, C_6D_6): δ 205 (bs) (prepared from $[Ta(^{13}CO)_2(dmpe)_2Cl]$). ^{31}P NMR (121 MHz, C_6D_6): δ 32.2. Anal. Calcd for $C_{26}H_{58}F_3O_5P_4SSiTa$: C, 35.78; H, 6.70; N, 0.00. Found: C, 35.82; H, 6.48; N, 0.00.

$[Ta(COSi^tBuPh_2)(CO)(depe)_2]$ (2). A 25-mL, one-necked, pear-shaped flask fitted with a rubber septum was charged with $[Ta(CO)_2(depe)_2Cl]$ (0.212 g, 0.31 mmol) and 10 mL of THF. Upon dissolution, excess 40% sodium amalgam was added and the reaction mixture was stirred vigorously for 3.5 h. The solution was decanted into a second 25-mL, one-necked, pear-shaped flask, and $^tBuPh_2SiCl$ (0.081 mL, 0.085 g, 0.31 mmol) was added in one portion via syringe, resulting in a deep red solution. The reaction mixture was stirred for an additional 0.75 h, after which the solvents were removed under vacuum, the product was extracted with pentane, and the pentane solution was filtered and concentrated, providing the crude product as a red oil. Crystallization from pentane at −30 °C afforded 0.220 g (80%) of **2** as a red solid. An analytically pure sample was obtained by recrystallization from TMS at −30 °C. IR (Nujol): 1786, 1418, 1291, 1263, 1245, 1114, 1027, 863, 822, 811, 758, 700 cm^{-1}. ^1H NMR (300 MHz, C_6D_6): δ 8.21 (m, 2 H), 7.98 (m, 2 H), 7.47 (t, J = 6.8 Hz, 2 H), 7.34 (m, 4 H), 2.15 (m, 2 H), 0.8−1.9 (m, 43 H), 1.26 (s, 9 H), 0.64 (dt, J = 7.4, 12.7 Hz, 3 H). ^{31}P NMR (121 MHz, C_6D_6): δ 48.5, 48.1, 36.1, 21.4. Anal. Calcd for $C_{38}H_{67}O_2P_4SiTa$: C, 51.35; H, 7.60; N, 0.00. Found: C, 51.02; H, 7.60; N, 0.00.

$[Ta(EtOC{\equiv}COSi^tBuPh_2)(depe)_2OTf]$ (3a). A 25-mL, one-necked, pear-shaped flask fitted with a rubber septum was charged with $[Ta(CO)_2(depe)_2Cl]$ (0.205 g, 0.30 mmol) and 10 mL of THF. Upon dissolution, excess 40% sodium amalgam was added and the reaction mixture was stirred vigorously for 4.6 h. The solution was decanted into a second 25-mL, one-necked, pear-shaped flask, and $^tBuPh_2SiCl$ (0.078 mL, 0.082 g, 0.30 mmol) was added in one portion via syringe, resulting in a deep red solution. The reaction mixture was stirred for an additional 1 h, after which the solvents were removed under vacuum, the product was extracted with pentane, and the pentane solution was filtered and concentrated, providing a red oil (0.253 g), unpurified $[Ta(COSi^tBuPh_2)(CO)(depe)_2]$. A 25-mL, one-necked, pear-shaped flask was charged with the crude carbyne and 7 mL of DME. Upon dissolution, ethyl triflate (0.035 mL, 0.048 g, 0.27 mmol) was added in one portion and the reaction mixture was stirred for 2.5 h. Upon removal of the solvents under vacuum, the product was extracted with pentane and the pentane solution was filtered and concentrated under vacuum to provide a gummy green solid. After trituration with pentane, recrystallization from pentane at −30 °C afforded 0.176 g (55% for two steps) of green crystalline **3a**. IR (Nujol): 1623, 1427, 1322, 1233, 1205, 1168, 1107, 1020, 973, 869, 730, 701 cm^{-1}. ^1H NMR (300 MHz, C_6D_6): δ 7.58−7.61 (m, 4 H), 7.12−7.14 (m, 6 H), 2.79 (q, J = 7.0 Hz, 2 H), 2.11−2.22 (m, 4 H), 1.71−2.04 (m, 18 H), 1.02−1.17 (m, 26 H), 1.05 (s, 9 H), 0.31 (t, J = 7.0 Hz, 3 H). ^{31}P NMR (121 MHz, C_6D_6): δ 52.8. Anal. Calcd for $C_{41}H_{72}F_3O_5P_4SSiTa$: C, 46.15; H, 6.80; N, 0.00. Found: C, 46.54; H, 6.77; N, 0.00.

$[Ta(EtOC{\equiv}COSiPh_3)(depe)_2OTf]$ (3b). A 25-mL, one-necked, pear-shaped flask fitted with a rubber septum was charged with $[Ta(CO)_2(depe)_2Cl]$ (0.068 g, 0.12 mmol) and 5 mL of THF. Upon dissolution, excess 40% sodium amalgam was added and the reaction mixture was stirred vigorously for 3.5 h. The solution was decanted into a second 25-mL, one-necked, pear-shaped flask, and Ph_3SiCl (0.029 g, 0.10 mmol) was added in one portion via syringe, resulting in a deep red solution. The reaction mixture was stirred for an additional 1 h, after which the solvents were removed under vacuum, the product was extracted with pentane, and the pentane solution was filtered and concentrated, providing a red oil (0.084 g), unpurified $[Ta(COSiPh_3)(CO)(depe)_2]$. A 25-mL, one-necked, pear-shaped flask was charged with the unpurified carbyne and 5 mL of DME and cooled to −30 °C. Upon dissolution, ethyl triflate (0.012 mL, 0.016 g, 0.09 mmol) was added in one portion and the reaction mixture was stirred for 0.5 h. Upon removal of the solvents under vacuum, the product was extracted with pentane and the pentane solution was filtered and concentrated under vacuum to provide a gummy green solid. After trituration with pentane, recrystallization from pentane at −30 °C afforded 0.018 g (14% for two steps) of green crystalline **3b**. IR (Nujol): 1622, 1428, 1317, 1230, 1208, 1167, 1114, 1102, 1084, 1019, 982, 870, 806, 732 cm^{-1}. ^1H NMR (300 MHz, C_6D_6): δ 7.57−7.60 (m, 6 H), 7.10−7.19 (m, 9 H), 3.27 (q, J = 7.0 Hz, 2 H), 1.58−2.10 (m, 22 H), 1.00−1.24 (m, 26 H), 0.54 (t, J = 7.0 Hz, 3 H). ^{31}P NMR (121 MHz, C_6D_6): δ 51.1. Anal. Calcd for $C_{43}H_{68}F_3O_5P_4SSiTa$: C, 47.51; H, 6.31; N, 0.00. Found: C, 47.98; H, 5.93; N, 0.00.

(38) Protasiewicz, J. D.; Bianconi, P. A.; Williams, I. D.; Liu, S.; Rao, C. P.; Lippard, S. J. *Inorg. Chem.* **1992**, *31*, 4134.

[Ta(EtOC≡COSiMe$_3$)(depe)$_2$OTf] (3c). A 25-mL, one-necked, pear-shaped flask fitted with a rubber septum was charged with [Ta(CO)$_2$(depe)$_2$Cl] (0.103 g, 0.15 mmol) and 8 mL of THF. Upon dissolution, excess 40% sodium amalgam was added and the reaction mixture was stirred vigorously for 4 h. The solution was decanted into a second 25-mL, one-necked, pear-shaped flask, and Me$_3$SiCl (0.019 mL, 0.016 g, 0.15 mmol) was added in one portion via syringe, resulting in a deep red solution. The reaction mixture was stirred for an additional 30 min, after which the solvents were removed under vacuum. The product was extracted with pentane, and the pentane solution was filtered and concentrated, providing a red oil (0.108 g), unpurified [Ta(COSiMe$_3$)(CO)(depe)$_2$]. A 25-mL, one-necked, pear-shaped flask was charged with the unpurified carbyne and 5 mL of DME. With rapid stirring, EtOTf (0.019 mL, 0.027 g, 0.15 mmol) was added in one portion and the reaction mixture was stirred for 1.5 h. After removal of the solvents under vacuum, the product was extracted with pentane and the pentane solution was filtered and concentrated under vacuum to provide a green-brown solid. Recrystallization from pentane at −30 °C afforded **3c** (0.031 g, 23%) as green crystals. IR (Nujol): 1591, 1324, 1202, 1167, 1036, 1016, 988, 841, 723 cm^{-1}. ^{1}H NMR (300 MHz, C$_6$D$_6$): δ 3.68 (q, J = 7.0 Hz, 2 H), 1.97−2.14 (m, 8 H), 1.71−1.86 (m, 12 H), 1.53−1.61 (m, 4 H), 0.97−1.12 (m, 24 H), 0.99 (t, J = 7.0 Hz, 3 H), 0.05 (s, 9 H). ^{31}P NMR (121 MHz, C$_6$D$_6$): δ 50.2.

[Ta(AcOC≡COSi^{t}BuPh$_2$)(depe)$_2$Cl] (4). A 25-mL, one-necked, pear-shaped flask fitted with a rubber septum was charged with [Ta(COSi^{t}BuPh$_2$)(CO)(depe)$_2$] (0.088 g, 0.1 mmol) and 5 mL of DME. Upon dissolution, the reaction vessel was cooled to −30 °C, acetyl chloride (0.007 mL, 0.008 g, 0.08 mmol) was added in one portion via syringe, and the reaction mixture was stirred for 10 min, providing a green solution. The solvents were removed under vacuum, the product was extracted with pentane, and the pentane solution was filtered and concentrated under vacuum to afford 0.084 g of the crude product as a green solid. Recrystallization from pentane at −30 °C provided 0.062 g (64%) of **4** as green crystals. IR (Nujol): 1723, 1538, 1365, 1234, 1227, 1114, 1083, 1031, 1019, 964, 927, 868, 804, 757, 722 cm^{-1}. ^{1}H NMR (300 MHz, C$_6$D$_6$): δ 7.68−7.71 (m, 4 H), 7.18−7.20 (m, 6 H), 1.81−2.10 (m, 16 H), 1.62−1.67 (m, 8 H), 1.07−1.22 (m, 24 H), 1.17 (s, 9 H), 1.12 (s, 3 H). ^{31}P NMR (121 MHz, C$_6$D$_6$): δ 43.0. Anal. Calcd for C$_{40}$H$_{70}$ClO$_3$P$_4$SiTa: C, 49.66; H, 7.29; N, 0.00. Found: C, 49.35; H, 7.20; N, 0.00.

[Ta(AcOC≡COSi^{t}BuPh$_2$)(dmpe)$_2$Cl] (5). A 25-mL, one-necked, pear-shaped flask fitted with a rubber septum was charged with [Ta(COSi^{t}BuPh$_2$)(CO)(dmpe)$_2$] (0.078 g, 0.1 mmol) and 5 mL of DME. Upon dissolution, the reaction vessel was cooled to −30 °C, acetyl chloride (0.007 mL, 0.008 g, 0.08 mmol) was added in one portion via syringe, and the reaction mixture was stirred for 15 min, providing a green solution. The solvent was removed under vacuum, the product was extracted with pentane, and the pentane solution was filtered and concentrated under vacuum to afford 0.072 g of the crude product as a green solid. Recrystallization from pentane at −30 °C provided 0.044 g (51%) of **5** as a green solid. IR (Nujol): 1724, 1540, 1430, 1365, 1291, 1276, 1234, 1113, 1098, 1033, 979, 938, 929, 889, 821, 794, 744, 731, 699 cm^{-1}. ^{1}H NMR (300 MHz, C$_6$D$_6$): δ 7.64−7.67 (m, 4 H), 7.13−7.16 (m, 6 H), 1.52−1.72 (m, 8 H), 1.52 (m, 12 H), 1.41 (m, 12 H), 1.12 (s, 9 H), 1.01 (s, 3 H). ^{31}P NMR (121 MHz, C$_6$D$_6$): δ 26.4. Anal. Calcd for C$_{32}$H$_{54}$ClO$_3$P$_4$SiTa: C, 44.95; H, 6.36; N, 0.00. Found: C, 44.39; H, 6.08; N, 0.00.

[Nb(AcOC≡COSi^{t}BuPh$_2$)(dmpe)$_2$Cl] (6). A 25-mL, one-necked, pear-shaped flask fitted with a rubber septum was charged with [Nb(CO)$_2$(dmpe)$_2$Cl] (0.048 g, 0.10 mmol) and 10 mL of THF. Upon dissolution, excess 40% sodium amalgam was added and the reaction mixture was stirred vigorously for 3.5 h. The solution was decanted into a second 25-mL, one-necked, pear-shaped flask, and ^{t}BuPh$_2$SiCl (0.026 mL, 0.027 g, 0.10 mmol) was added in one portion via syringe, resulting in a deep red solution. The reaction mixture was stirred for an additional 1 h, after which the solvents were removed under vacuum, the product was extracted with pentane, and the pentane solution was filtered and concentrated, providing unpurified [Nb(COSi^{t}BuPh$_2$)(CO)(dmpe)$_2$] as a red oil (0.068 g). A 25-mL, one-necked, pear-shaped flask fitted with a rubber septum was charged with the unpurified [Nb(COSi^{t}BuPh$_2$)(CO)(dmpe)$_2$] and 5 mL of DME. Upon dissolution, the reaction vessel was cooled to −30 °C, acetyl chloride (0.007 mL, 0.008 g, 0.08 mmol) was added in one portion via syringe, and the reaction mixture was stirred for 10 min, providing a green solution. The solvent was removed under vacuum, the product was extracted with pentane, and the pentane solution was filtered and concentrated under vacuum to afford the product as a green solid. Recrystallization from pentane at −30 °C provided 0.031 g (40%) of **6** as a green solid. IR (Nujol): 1725, 1544, 1430, 1365, 1292, 1280, 1232, 1113, 1095, 1032, 979, 938, 929, 890, 821, 791, 744, 730, 700 cm^{-1}. ^{1}H NMR (300 MHz, C$_6$D$_6$): δ 7.62−7.65 (m, 4 H), 7.11−7.15 (m, 6 H), 1.55−1.80 (m, 8 H), 1.40 (t, J = 2.7 Hz, 12 H), 1.35 (t, J = 2.7 Hz, 12 H), 1.13 (s, 9 H), 1.02 (s, 3 H). Anal. Calcd for C$_{32}$H$_{54}$ClO$_3$P$_4$SiNb: C, 50.10; H, 7.10; N, 0.00. Found: C, 50.29; H, 6.90; N, 0.00.

[Ta(MeO$_2$COC≡COSi^{t}BuPh$_2$)(dmpe)$_2$Cl] (7). A 25-mL, one-necked, pear-shaped flask fitted with a rubber septum was charged with [Ta(COSi^{t}BuPh$_2$)(CO)(dmpe)$_2$] (0.038 g, 0.05 mmol) and 5 mL of THF. Upon dissolution, methyl chloroformate (0.004 mL, 0.005 g, 0.05 mmol) was added in one portion via syringe and the reaction mixture was stirred for 1 h, providing a green solution. The solvents were removed under vacuum, the product was extracted with pentane, and the pentane solution was filtered and concentrated under vacuum to afford the product as a green solid. Recrystallization from pentane at −30 °C provided 0.031 g (71%) of **7** as a green solid. IR (Nujol): 1738, 1560, 1425, 1366, 1292, 1277, 1254, 1114, 1074, 1020, 973, 941, 927, 889, 829, 802, 748, 733, 699 cm^{-1}. ^{1}H NMR (300 MHz, C$_6$D$_6$): δ 7.71−7.74 (m, 4 H), 7.10−7.17 (m, 6 H), 2.93 (s, 3 H), 1.51−1.68 (m, 8 H), 1.48 (s, 12 H), 1.39 (s, 12 H), 1.16 (s, 9 H). ^{31}P NMR (121 MHz, C$_6$D$_6$): δ 26.1. Anal. Calcd for C$_{32}$H$_{54}$ClO$_4$P$_4$SiTa: C, 44.12; H, 6.25; N, 0.00. Found: C, 44.23; H, 6.19; N, 0.00.

[V(η^2-C(O)Et)(CO)(dmpe)$_2$] (8). To a stirred solution of Na[V(CO)$_2$(dmpe)$_2$] (0.155 g, 0.360 mmol) in 10 mL of DME was added Et$_3$OBF$_4$ (0.072 g, 0.380 mmol). The solution turned immediately dark brown-black. After the solution was stirred for several minutes, the solvent was removed under vacuum, leaving a red-brown material which was extracted into a few milliliters of pentane. Cooling the solution to −30 °C yielded a mixture of red crystals ([V(CO)$_2$(dmpe)$_2$], identified by FTIR) and very dark brown crystals of **8**, which were collected by filtration and dried (0.079 g). ^{1}H NMR (300 MHz, C$_6$D$_6$): δ 3.39 (m), 3.24 (m), 1.80 (bs), 1.58 (bs), 1.41 (bs), 1.27 (bs), 0.71 (bs), 0.62 (bs). ^{31}P NMR (121 MHz, C$_6$D$_6$): δ 71 (m), 40−58 (m, two overlapping signals), 29 (m).

[Ta(AcOC≡COAc)(dmpe)$_2$Cl] (9). A 25-mL, one-necked, pear-shaped flask fitted with a rubber septum was charged with [Ta(CO)$_2$(dmpe)$_2$Cl] (0.115 g, 0.2 mmol) and 10 mL of DME. Upon dissolution, excess 40% sodium amalgam was added in one portion and the reaction mixture was stirred vigorously for 4 h. The orange solution was decanted into a second 25-mL, one-necked, pear-shaped flask fitted with a rubber septum, the reaction vessel was cooled to −30 °C, and acetyl chloride (0.028 mL, 0.031 g, 0.4 mmol) was added in one portion via syringe. The reaction mixture was stirred for 2 min, providing a green solution. Upon removal of the solvents under vacuum, the green product was extracted with pentane and the pentane solution was filtered and concentrated under vacuum to provide a green solid. Recrystallization from pentane at −30 °C yielded 0.063 g (48%) of **9** as green crystals. IR (Nujol): 1742, 1566, 1420, 1361, 1293, 1282, 1216, 1088, 1008, 943, 925, 891, 733, 699 cm^{-1}. ^{1}H NMR (300 MHz, C$_6$D$_6$): δ 1.82 (s, 6 H), 1.50−1.61 (m, 16 H), 1.23−1.44 (m, 16

H). ^{13}C NMR (75.5 MHz, C_6D_6): δ 200.4 (p, J = 14.7 Hz) (**9b**, prepared from [Ta(^{13}CO)$_2$(dmpe)$_2$Cl]). ^{31}P NMR (121 MHz, C_6D_6): δ 24.5. Anal. Calcd for $C_{18}H_{38}ClO_4P_4Ta$: C, 32.82; H, 5.81; N, 0.00. Found: C, 32.67; H, 5.90; N, 0.00. Spectral data for material prepared from 99% $CH_3{}^{13}C(O)Cl$, [Ta($CH_3C^*(O)OC{\equiv}COC^*(O)CH_3$)(dmpe)$_2$Cl] (**9a**): IR (Nujol) 1702, 1564, 1421, 1360, 1293, 1282, 1186, 1085, 1007, 942, 924, 890, 836, 733, 699 cm^{-1}; ^1H NMR (300 MHz, C_6D_6) δ 1.82 (d, J = 6.3 Hz, 6 H), 1.50−1.61 (m, 16 H), 1.23−1.44 (m, 16 H); ^{13}C NMR (75.5 MHz, C_6D_6) δ 166.6.

[Ta(AcOC≡COAc)(depe)$_2$Cl] (10). A 25-mL, one-necked, pear-shaped flask fitted with a rubber septum was charged with [Ta(CO)$_2$(depe)$_2$Cl] (0.068 g, 0.1 mmol) and 10 mL of DME. Upon dissolution, excess 40% sodium amalgam was added in one portion and the reaction mixture was stirred vigorously for 3 h. The orange solution was decanted into a second 25-mL, one-necked, pear-shaped flask fitted with a rubber septum, the reaction vessel was cooled to −30 °C, and acetyl chloride (0.014 mL, 0.016 g, 0.2 mmol) was added in one portion via syringe. The reaction mixture was stirred for 15 min, providing a green solution. Upon removal of the solvents under vacuum, the green product was extracted with pentane and the pentane solution was filtered and concentrated under vacuum to provide a green solid. Recrystallization from pentane at −30 °C yielded 0.033 g (43%) of **10** as green crystals. IR (Nujol): 1749, 1569, 1419, 1365, 1211, 1080, 1030, 1008, 965, 869, 807, 761, 728 cm^{-1}. ^1H NMR (300 MHz, C_6D_6): δ 1.83−2.01 (m, 16 H), 1.83 (s, 6 H), 1.63−1.67 (m, 4 H), 1.39−1.43 (m, 4 H), 1.01−1.18 (m, 24 H). ^{31}P NMR (121 MHz, C_6D_6): δ 41.5. Anal. Calcd for $C_{26}H_{54}ClO_4P_4Ta$: C, 40.50; H, 7.06; N, 0.00. Found: C, 40.50; H, 7.00; N, 0.00. Spectral data for material prepared from 99% $CH_3{}^{13}C(O)Cl$, [Ta($CH_3C^*(O)OC{\equiv}COC^*(O)CH_3$)(depe)$_2$Cl] (**10a**): IR (Nujol) 1709, 1567, 1415, 1365, 1183, 1080, 1037, 1006, 963, 866, 807, 727 cm^{-1}; ^1H NMR (300 MHz, C_6D_6): δ 1.83−2.03 (m, 16 H), 1.83 (d, J = 7.1 Hz, 6 H), 1.62−1.69 (m, 4 H), 1.36−1.42 (m, 4 H) 1.01−1.18 (m, 24 H); ^{13}C NMR (75.5 MHz, C_6D_6) δ 166.8.

X-ray Crystallography. [Ta(AcOC≡COSi^{t}BuPh$_2$)(depe)$_2$Cl] (4). Green crystals were grown by cooling a saturated solution of **4** in pentane at −30 °C. The crystals were removed from the glovebox in a pool of Exxon Paratone-N oil to minimize decomposition. An irregularly shaped crystal (dimensions 0.35 × 0.38 × 0.43 mm) was cut from a larger specimen and mounted with silicon grease on the end of a quartz fiber. Unit cell parameters and intensity data were obtained by standard methods in our laboratory, details of which are provided in Table 1. The crystal was judged to be acceptable on the basis of open counter ω-scans of several low-angle reflections ($\Delta\bar{\omega}_{1/2}$ = 0.24°) and by axial photographs. The tantalum atom was located by the SIR-92[39] direct methods option in the teXsan software package.[40] The remaining non-hydrogen atoms were revealed by initial cycles of DIRDIF[41] followed by alternating least-squares refinements and difference Fourier maps. All non-hydrogen atoms were refined anisotropically, except for the carbon atoms C300−C305 of the phenyl ring, which were treated as a rigid group. This ring and an ethyl group (C34 and C35) were disordered over two positions. The site occupancies of the latter were refined, resulting in a 70/30 population distribution. The populations of the two ethyl sites were fixed, and then this same distribution was applied to the phenyl ring positions. Hydrogen atoms were placed at calculated positions in the final refinement cycles. The largest residual peak in the final difference Fourier map was 1.49 e/Å^3 near the tantalum atom.

[V(η^2-C(O)Et)(CO)(dmpe)$_2$] (8). Very dark brown crystals of **8** and light red crystals of *trans*-[V(CO)$_2$(dmpe)$_2$] were grown from a mixture of the two complexes in pentane at −30 °C. A crystal of dimensions 0.20 × 0.20 × 0.20 mm was mounted from a cold stage onto the end of a quartz fiber with silicon grease. Unit cell parameters and intensity data were obtained by standard methods, details of which are provided in Table 1. The crystal was judged to be acceptable on the basis of open counter ω-scans of several low-angle reflections ($\Delta\bar{\omega}_{1/2}$ = 0.24°). The vanadium atom positional parameters were determined by the SHELXS-86[42] option in the TEXSAN[43] structure solution package. The remaining non-hydrogen atoms were located by iterations of the DIRDIF[41] program followed by subsequent least-squares refinements and difference Fourier maps. All non-hydrogen atoms were refined anisotropically. Hydrogen atoms were placed at calculated positions in the final refinement cycles. The largest residual peak in the final difference Fourier map was 0.38 e/Å^3 located near the vanadium atom.

Table 1. Experimental Details of the X-ray Diffraction Studies of [Ta(AcOC≡COSi^{t}BuPh$_2$)(depe)$_2$Cl] (4), [V(η^2-C(O)Et)(CO)(dmpe)$_2$] (8), and [Ta(AcOC≡COAc)(dmpe)$_2$Cl] (9)[a]

	4	8	9
empirical formula	$C_{40}H_{70}O_3P_4SiTaCl$	$C_{16}H_{37}O_2P_4V$	$C_{18}H_{38}O_4P_4TaCl$
fw	967.37	436.3	658.79
a, Å	21.553(5)	12.917(2)	14.964(2)
b, Å	10.893(1)	14.331(2)	11.960(2)
c, Å	20.213(2)	12.335(2)	31.710(5)
β, deg	117.86(2)	90	102.77(1)
V, Å^3	4569(2)	2283.4(6)	5535(1)
T, °C	−110	−78	−60
Z	4	4	8
ϱ_{calc}, g cm^{-3}	1.41	1.27	1.58
space group	$P2_1/n$	$Pna2_1$	$C2$
2θ limits, deg	3−50	3−48	3−46
data limits	$-h,-k,\pm l$	$+h,+k,+l$	$+h,+k,\pm l$
scan type	$\omega/2\theta$	$\omega/2\theta$	$\omega/2\theta$[b]
μ, cm^{-1}	26.6	7.0	43.1
no. of total data	8838	2658	6084
no. of unique data[c]	6034	2067	4069
no. of params	427	207	407
p factor	0.05	0.03	0.03
abs corr	empirical (ψ)		empirical (ψ)
transmissn range	0.818−1.00	0.956−1.00	0.826−1.00
R_{merge}	0.025	0.032	0.096
GOF	1.810	1.21	1.898
R[d]	0.041	0.040	0.063
R_w	0.044	0.044	0.071

[a] Data were collected on an Enraf-Nonius CAD-4F κ geometry diffractometer using Mo Kα radiation. [b] This choice of scan type may have led to some reflection overlap, diminishing the accuracy of the data. [c] Observation criterion $I > 3\sigma(I)$. [d] $R = \sum||F_o| - |F_c||/\sum|F_o|$ and $R_w = [\sum w(|F_o| - |F_c|)^2/\sum w|F_o|^2]^{1/2}$, where $w = 1/\sigma^2(F)$, as defined in: Carnahan, E. M.; Rardin, R. L.; Bott, S. G.; Lippard, S. J. *Inorg. Chem.* **1992**, *31*, 5193.

[Ta(AcOC≡COAc)(dmpe)$_2$Cl] (9). Green crystals were grown by cooling a saturated solution of **9** in pentane at −30 °C. An irregularly shaped crystal (dimensions 0.35 × 0.38 × 0.43 mm) was cut from a larger specimen, coated with Exxon Paratone-N oil, and mounted on the end of a quartz fiber with silicon grease. Unit cell and data collection parameters are summarized in Table 1. The crystal was judged to be acceptable on the basis of open counter ω-scans of several low-angle reflections ($\Delta\bar{\omega}_{1/2}$ = 0.29°) and by axial photographs. The tantalum atom was located by direct methods. The remaining non-hydrogen atoms were revealed by subsequent least-squares refinements and difference Fourier maps. Anisotropic refinement of non-hydrogen atoms produced several non-positive-definite temperature factors, and some bond distances

(39) Altomare, A.; Burla, M. C.; Camalli, M.; Cascarano, G.; Giacovazzo, C.; Guagliardi, A.; Polidori, G. *J. Appl. Crystallogr.* **1994**, *27*, 435.
(40) *TeXsan: Single Crystal Structure Analysis Software, Version 1.6c*; Molecular Structure Corp.: The Woodlands, TX, 1994.
(41) Parthasarathi, V.; Beurskens, P. T.; Slot, H. J. B. *Acta Crystallogr.* **1983**, *A39*, 860.
(42) Sheldrick, G. M. In *Crystallographic Computing*; Sheldrick, G. M., Krüger, C., Goddard, R. Eds.; Oxford University Press: Oxford, U.K., 1985; p 175.
(43) *TEXSAN: Single Crystal Structure Analysis Software, Version 5.0*; Molecular Structure Corp.: The Woodlands, TX, 1989.

and angles for the two independent molecules in the asymmetric unit were inconsistent with one another. This inconsistency persisted irrespective of whether or not the absorption and decay corrections were applied, and whether refinement was carried out using F or F^2. Attempts to solve the structure in the alternative space groups Cm or $C2/m$ were not successful, and packing diagrams were consistent only with $C2$ as the space group. Although the unit cell contains both enantiomers, they are not related by a crystallographic symmetry element. The choice of polarity was made following refinement with both orientations. The largest residual peak in the final difference Fourier mp was 1.94 e/Å^3, situated near Ta1.

Results and Discussion

Siloxycarbyne–CO Coupling. Previous work demonstrated that siloxycarbynes of the type [M(≡COSiR$_3$)(CO)(dmpe)$_2$] react with a variety of silylating reagents (R'$_3$SiX) to afford the corresponding coupled products [M(R$_3$SiOC≡COSiR'$_3$)(dmpe)$_2$X]. More recently, we have shown that addition of AlEt$_3$ to [Ta(≡COSi^{t}BuPh$_2$)(CO)(dmpe)$_2$] produces the unusual carbene–carbyne species [Ta(≡COSi^{t}BuPh$_2$)(=C=O-AlEt$_3$)(dmpe)$_2$].[13,24] Attempts to add nucleophiles (Nu) to this species to promote C–C bond formation and yield products of the kind [M(R$_3$SiOC≡COAlEt$_3$)(CO)(dmpe)$_2$-Nu] have thus far not resulted in carbene–carbyne coupling, but rather in removal of AlEt$_3$ to regenerate [Ta(≡COSi^{t}BuPh$_2$)(CO)(dmpe)$_2$]. These results suggested that the carbyne–CO coupling process depends on the nature of the electrophile and led us to expand the range of electrophiles that might result in O-alkylation of the CO ligand in [M(≡COSiR$_3$)(CO)-(dmpe)$_2$]. Since the bond angle between the coordinated carbon atoms of the carbene and carbyne ligands in [Ta-(≡COSi^{t}BuPh$_2$)(=C=OAlEt$_3$)(dmpe)$_2$] decreased to 73.4-(4)° from its value of 88.5(6)° in [Ta(≡COSi^{t}BuPh$_2$)-(CO)(dmpe)$_2$], we were interested to know whether O-alkylation by a carbon-based electrophile would generate the [Ta(≡COSiR$_3$)(=C=OR')(dmpe)$_2$]$^+$ analogue or possibly lead to coupled products [M(R$_3$SiOC≡COR')-(CO)(dmpe)$_2$]$^+$ or [M(R$_3$SiOC≡COR')(CO)(dmpe)$_2$X].

Reactions of [Ta(≡COSi^{t}BuPh$_2$)(CO)(dmpe)$_2$] with a series of alkylating reagents were therefore investigated. Addition of Et$_3$OBF$_4$, BnBr, or allyl iodide to [Ta(≡COSi^{t}BuPh$_2$)(CO)(dmpe)$_2$] produced yellow solutions, signaling oxidation to [Ta(CO)$_2$(dmpe)$_2$X] species. Analysis of the IR spectra of the yellow solids isolated from the reaction mixtures confirmed the presence of two *cis*-CO ligands, whereas ^{1}H NMR spectroscopy indicated the absence of resonances attributable to metal alkyls. In this manner, we identified the capping ligands (X) in these [Ta(CO)$_2$(dmpe)$_2$X] complexes as halide ion. Similar results were obtained irrespective of the solvents or reaction temperatures employed. Reaction of MeOTf with [Ta(≡COSi^{t}BuPh$_2$)(CO)(dmpe)$_2$], however, provided [Ta(CO)$_2$(dmpe)$_2$Me], as revealed by the characteristic Ta–Me signal in the ^{1}H NMR spectrum at −1.59 ppm.[26]

Very different results were obtained when DME solutions of [Ta(≡COSi^{t}BuPh$_2$)(CO)(dmpe)$_2$] were treated with ethyl triflate. The deep red color of the carbyne complex changed to green-brown, mimicking the well-established behavior of silyl-induced coupling processes. Removal of solvent and extraction of the product mixture with pentane led to isolation of a green-brown compound that was recrystallized as brown crystals from pentane. Analysis of the IR spectrum of this new complex showed no terminal CO stretches and a new band at 1609 cm^{-1}, which was assigned to the acetylene ligand in [Ta(EtOC≡COSi^{t}BuPh$_2$)(dmpe)$_2$OTf] (**1a**). The ^{31}P NMR spectrum consisted of a single resonance at 34.2 ppm, as observed in other four-electron-donor acetylene complexes.[44] A similar product, [Ta-(EtOC≡COSi^{i}Pr$_3$)(dmpe)$_2$OTf] (**1b**), was isolated from the reaction of [Ta(≡COSi^{i}Pr$_3$)(CO)(dmpe)$_2$] with ethyl triflate, although the yields of both **1a** and **1b** were somewhat lower than for analogous reactions with silyl reagents (eq 2).

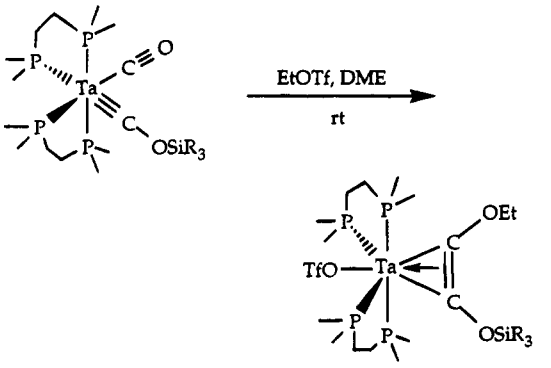

(2)

Analogous siloxy–ethoxy acetylene complexes could be prepared from complexes containing the chelating phosphine ligand depe. Addition of EtOTf to a DME solution of [Ta(≡COSi^{t}BuPh$_2$)(CO)(depe)$_2$] afforded [Ta(EtOC≡COSi^{t}BuPh$_2$)(depe)$_2$OTf] (**3a**) in slightly higher yields. Longer reaction times were required, presumably owing to the increased steric bulk about the metal center. Similarly, the (triphenylsiloxy)- and (trimethylsiloxy)carbynes [Ta(≡COSiPh$_3$)(CO)(depe)$_2$] and [Ta(≡COSiMe$_3$)(CO)(depe)$_2$] reacted with EtOTf, yielding [Ta(EtOC≡COSiPh$_3$)(depe)$_2$OTf] (**3b**) and [Ta-(Me$_3$SiOC≡COEt)(depe)$_2$OTf] (**3c**), respectively (eq 3).

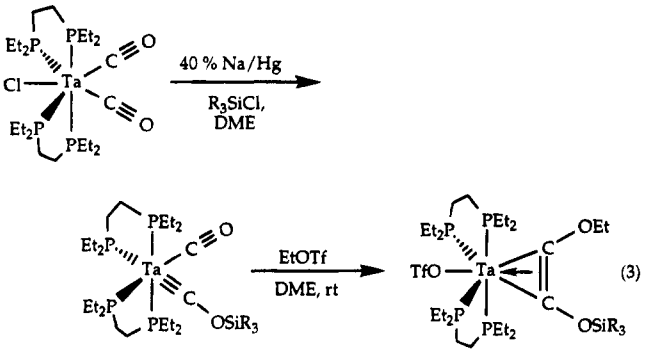

(3)

The ethylations proceeded in modest yields, ranging from 17 to 58%, indicating the lower propensity of the carbynes to couple with ethylating versus silylating reagents. Attempts to extend the reaction to larger alkylating reagents, such as ^{i}PrBr, led only to oxidized products, [M(CO)$_2$(dmpe)$_2$X]. Although the systems described above allowed for the first examples of carbyne–CO coupling, the reaction could not be achieved with a wider variety of electrophiles. To some extent, the reductive coupling reaction mimics the reactivity of

(44) Templeton, J. L. *Adv. Organomet. Chem.* **1989**, *29*, 1.

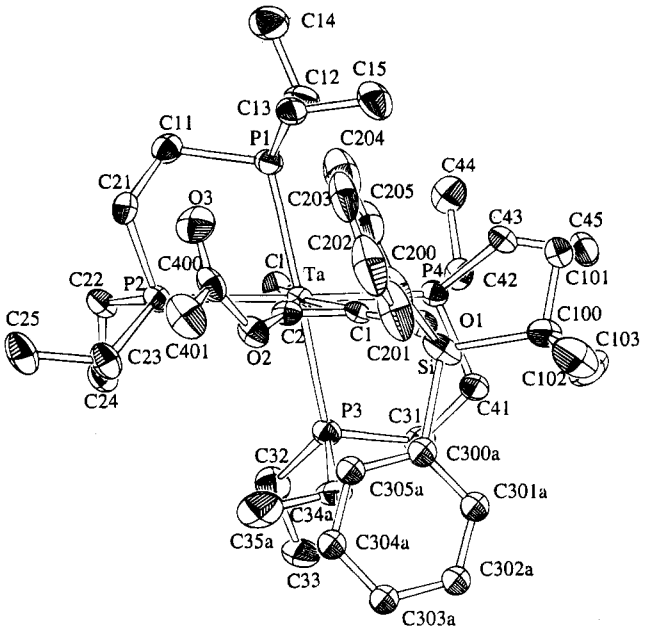

Figure 1. ORTEP diagram of [Ta(AcOC≡COSi^{t}BuPh$_2$)-(depe)$_2$Cl] (**4**) showing 40% thermal ellipsoids for all non-hydrogen atoms. The disordered atoms are shown at the sites of highest occupancy.

Scheme 3

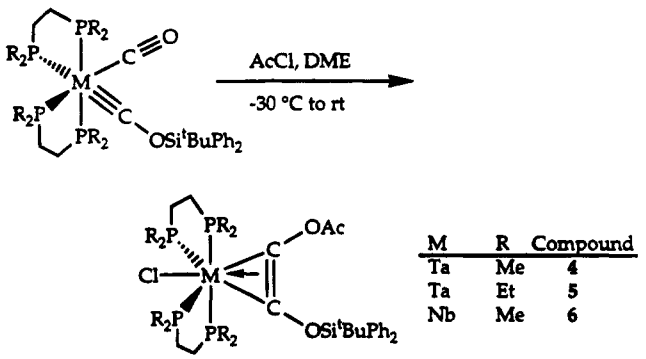

M	R	Compound
Ta	Me	4
Ta	Et	5
Nb	Me	6

enolates.[45] Trapping enolates as the corresponding silyl enol ethers is well-precedented, and these same silylating reagents afforded the best yields of reductively coupled products. In contrast, O-alkylation of enolates can be difficult,[46] a characteristic that applies to the carbyne–CO coupling reaction. These considerations prompted us to examine acyl chlorides, another reagent commonly employed to trap enolates as the corresponding enol ester.[47]

When acetyl chloride was added to a cooled solution of [Ta(≡COSi^{t}BuPh$_2$)(CO)(depe)$_2$] or [M(≡COSi^{t}BuPh$_2$)-(CO)(dmpe)$_2$] (M = Nb, Ta), the color changed to green, consistent with carbyne–CO coupling. Recrystallization from pentane afforded green crystals, the spectroscopic properties of which were consistent with the formation of [M(AcOC≡COSi^{t}BuPh$_2$)(depe or dmpe)$_2$Cl] (**4–6**) (Scheme 3). Most striking in the IR spectra are two bands at ca. 1724 and 1539 cm^{-1}. The more intense, higher energy mode can be assigned to the C=O stretch of the acetyl unit, whereas the lower energy band is ascribed to the bound acetylene ligand. The ^{31}P NMR spectra for **4** and **5** displayed characteristic singlets at 43.0 and 25.4 ppm, respectively.

X-ray analysis of **4** revealed the geometry of the reductively coupled product in the solid state (Figure 1). This compound is the first structurally characterized product resulting from carbyne–CO coupling on a group V metal center with carbon-based electrophiles. The geometry of the seven-coordinate complex is very similar to that of niobium and tantalum complexes prepared by reductive coupling of carbon monoxide ligands with the use of silyl reagents. Tables 2 and 3 list fractional

Table 2. Positional Parameters and Equivalent Isotropic Thermal Parameters for the Non-Hydrogen Atoms in [Ta(AcOC≡COSi^{t}BuPh$_2$)(depe)$_2$Cl] (4)[a]

atom	*x*	*y*	*z*	*B*(eq), Å^2 [b]
Ta	0.28380(2)	0.18380(3)	0.60311(1)	2.07(1)
Cl	0.2938(1)	0.2373(2)	0.7190(1)	3.05(7)
P1	0.2028(1)	0.3733(2)	0.5627(1)	2.70(8)
P2	0.3716(1)	0.3629(2)	0.6331(1)	2.57(7)
P3	0.3654(1)	0.0062(2)	0.6693(1)	2.63(7)
P4	0.1981(1)	0.0240(2)	0.6073(1)	2.41(7)
Si	0.2271(1)	−0.0733(2)	0.4012(1)	3.6(1)
O1	0.2232(2)	−0.0113(5)	0.4682(2)	2.6(2)
O2	0.3324(2)	0.1873(5)	0.4730(2)	3.1(2)
O3	0.2890(3)	0.3762(6)	0.4352(3)	4.6(3)
C1	0.2557(3)	0.0859(6)	0.5124(3)	2.0(3)
C2	0.2995(4)	0.1728(7)	0.5165(3)	2.4(3)
C11	0.2560(4)	0.5164(7)	0.5873(4)	3.1(3)
C12	0.1393(4)	0.4074(8)	0.5950(4)	3.9(4)
C13	0.1502(4)	0.3917(7)	0.4701(4)	3.4(3)
C14	0.1043(5)	0.533(1)	0.5773(5)	5.0(4)
C15	0.0906(4)	0.298(1)	0.4365(4)	4.9(4)
C21	0.3242(4)	0.4996(7)	0.5830(4)	3.5(3)
C22	0.4112(4)	0.4352(7)	0.7186(4)	3.1(3)
C23	0.4469(4)	0.352(1)	0.6152(4)	3.7(4)
C24	0.4642(4)	0.3582(8)	0.7772(4)	3.5(3)
C25	0.4925(4)	0.465(1)	0.6289(5)	4.9(4)
C31	0.3153(4)	−0.1166(7)	0.6851(4)	3.2(3)
C32	0.4383(4)	0.023(1)	0.7556(4)	4.5(4)
C33	0.4032(4)	−0.0780(8)	0.6231(4)	3.7(3)
C34a	0.4711(6)	−0.083(1)	0.7968(6)	4.6(6)
C34b	0.514(1)	0.062(3)	0.746(1)	5(1)
C35a	0.4601(7)	−0.006(1)	0.6177(7)	5.5(7)
C35b	0.444(1)	−0.200(3)	0.640(1)	3(1)
C41	0.2415(4)	−0.1295(7)	0.6246(4)	3.0(3)
C42	0.1707(4)	0.0246(7)	0.6749(4)	3.0(3)
C43	0.1147(3)	−0.0063(7)	0.5303(3)	2.7(3)
C44	0.1193(5)	0.1269(8)	0.6672(4)	4.2(4)
C45	0.0725(4)	−0.117(1)	0.5314(5)	4.5(4)
C100	0.1523(4)	−0.1849(8)	0.3654(4)	3.4(3)
C101	0.0845(4)	−0.1127(7)	0.3394(4)	3.6(3)
C102	0.1525(5)	−0.273(1)	0.4206(5)	5.7(4)
C103	0.1497(5)	−0.257(1)	0.3056(5)	6.1(5)
C200	0.2102(4)	0.042(1)	0.3347(4)	4.7(4)
C201	0.2245(5)	0.013(1)	0.2792(5)	6.6(5)
C202	0.2058(6)	0.090(1)	0.2261(6)	8.2(7)
C203	0.1722(5)	0.201(1)	0.2232(5)	5.9(5)
C204	0.1591(6)	0.234(1)	0.2780(6)	7.8(6)
C205	0.1787(5)	0.152(1)	0.3326(4)	5.2(4)
C400	0.3226(4)	0.289(1)	0.4358(4)	3.4(3)
C401	0.3599(5)	0.277(1)	0.3922(4)	5.1(4)
C300a	0.3142(3)	−0.1628(6)	0.4304(3)	2.9
C305a	0.3714(3)	−0.0954(4)	0.4351(3)	2.9
C304a	0.4361(3)	−0.1527(6)	0.4561(4)	2.9
C303a	0.4437(3)	−0.2774(6)	0.4723(4)	2.9
C302a	0.3865(3)	−0.3449(4)	0.4676(3)	2.9
C301a	0.3218(3)	−0.2876(6)	0.4466(3)	2.9
C300b	0.320(1)	−0.094(2)	0.418(1)	5.6
C305b	0.359(1)	−0.022(2)	0.395(1)	5.6
C304b	0.428(1)	−0.055(2)	0.412(1)	5.6
C303b	0.458(1)	−0.159(2)	0.452(1)	5.6
C302b	0.420(1)	−0.231(2)	0.474(1)	5.6
C301b	0.351(1)	−0.198(2)	0.457(1)	5.6

[a] Atoms are labeled as indicated in Figure 1. Estimated standard deviations in the least significant figure are given in parentheses. [b] $B(\text{eq}) = {}^4/_3[a^2\beta_{11} + b^2\beta_{22} + c^2\beta_{33} + 2ab(\cos\gamma)\beta_{12} + 2ac(\cos\beta)\beta_{13} + 2bc(\cos\alpha)\beta_{23}]$.

(45) Semmelhack, M. F.; Tamura, R. *J. Am. Chem. Soc.* **1983**, *105*, 4099.
(46) Tardella, P. A. *Tetrahedron Lett.* **1969**, 1117.
(47) Ladjama, D.; Riehl, J. J. *Synthesis* **1979**, 504.

Table 3. Selected Intramolecular Bond Distances (Å) and Angles (deg) Involving the Non-Hydrogen Atoms for [Ta(AcOC≡COSi^{t}BuPh$_2$)(depe)$_2$Cl] (4)[a]

	Bond Distances		
Ta–P1	2.579(2)	Ta–P2	2.580(2)
Ta–P3	2.562(2)	Ta–P4	2.570(2)
Ta–C1	2.088(7)	Ta–C2	2.090(8)
Ta–Cl	2.526(2)	C1–C2	1.31(1)
C1–O1	1.386(8)	C2–O2	1.44(1)
Si–O1	1.660(6)	C400–O2	1.33(1)
	Bond Angles		
Ta–C1–O1	152.5(6)	Ta–C2–O2	159.9(4)
C1–Ta–C2	36.6(3)	Si–O1–C1	135.7(5)
C400–O2–C2	120.9(7)	Cl–Ta–P2	82.00(7)
Cl–Ta–P1	83.56(7)	Cl–Ta–P4	81.01(7)
Cl–Ta–P3	83.56(7)	Cl–Ta–C2	163.9(2)
Cl–Ta–C1	160.1(1)	P1–Ta–P3	167.10(7)
P1–Ta–P2	77.31(7)	P1–Ta–C1	103.4(2)
P1–Ta–P4	99.94(7)	P2–Ta–P3	101.50(6)
P1–Ta–C2	95.9(2)	P2–Ta–C1	118.8(2)
P2–Ta–P4	162.99(7)	P3–Ta–P4	77.38(7)
P2–Ta–C2	82.2(2)	P3–Ta–C2	96.6(2)
P3–Ta–C1	88.5(2)	P4–Ta–C2	114.8(2)
P4–Ta–C1	78.2(2)	O2–C400–O3	126(1)
O2–C400–C401	110.0(8)	O3–C400–C401	123.8(9)

[a] Atoms are labeled as indicated in Figure 1. Estimated standard deviations in the least significant figure are given in parentheses.

coordinates and important distances and angles, respectively. The mean Ta–P bond length of 2.573(8) Å is elongated when compared to the mean value of 2.553(2) Å in [Ta(Me$_3$SiOC≡COSiMe$_3$)(dmpe)$_2$Cl],[7] although this difference in part reflects the choice of chelating phosphine ligand, since a similar difference occurs in the structures of [Ta(CO)$_2$(dmpe)$_2$Cl] (2.58(2) Å)[7] and [Ta(CO)$_2$(depe)$_2$Cl] (2.60(2) Å).[38] The C1–C2 bond distance of 1.31(1) Å is similar to the reported values for disiloxyacetylene ligands (1.31–1.33 Å).[5,13]

Methyl chloroformate was also used to induce the coupling of siloxycarbyne and CO ligands (eq 4). This

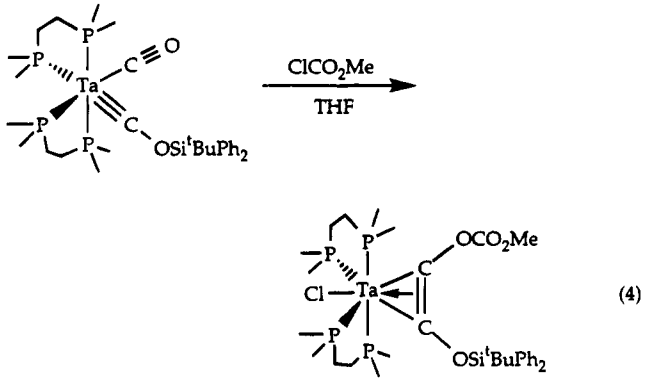

(4)

conversion proceeded at a much slower rate compared to reactions involving acetyl chloride and was best performed at room temperature. The spectroscopic properties of [Ta(MeO$_2$COC≡COSi^{t}BuPh$_2$)(dmpe)$_2$Cl] (**7**), notably the strong IR bands at 1738 and 1560 cm^{-1}, are similar to those in the acetyl chloride species described above.

Attempts to couple any of the siloxycarbyne complexes by addition of benzoyl chloride were unsuccessful, resulting instead in formation of the corresponding [M(CO)$_2$(R$_2$PCH$_2$CH$_2$PR$_2$)$_2$X] dicarbonyl species. Preliminary analysis of the products by IR spectroscopy indicated the presence of two CO stretches at 1829 and 1763 cm^{-1}.

Reactions of Dicarbonyl Anions with Alkylating Reagents. Having demonstrated that carbyne–CO coupling can be effected with carbon-based electrophiles, we were interested to determine whether coupling with such electrophiles could accomplished by starting with Na[M(CO)$_2$(dmpe)$_2$] (M = Nb, Ta). Irrespective of the reaction conditions employed, however, the predominant products resulting from the reaction of Na[M(CO)$_2$(dmpe)$_2$] or Na[M(CO)$_2$(depe)$_2$] (M = Nb, Ta) with alkylating agents, such as MeOTf and EtOTf, were metal–alkyl species, as determined by ^{1}H NMR spectroscopy. Similarly, the reaction of Na[V(CO)$_2$(dmpe)$_2$] with MeOTf afforded mixtures of [V(CO)$_2$(dmpe)$_2$Me] and [V(CO)$_2$(dmpe)$_2$].[48] Presumably, direct electrophilic attack of the alkylating reagent on the highly reduced metal center occurs for the Nb and Ta complexes, but electron-transfer reactions may be important for the vanadium complexes (see below).

Different results were obtained, however, when Na[V(CO)$_2$(dmpe)$_2$] was allowed to react either with EtOTf or Et$_3$OBF$_4$ (eq 5). A mixture of two products in com-

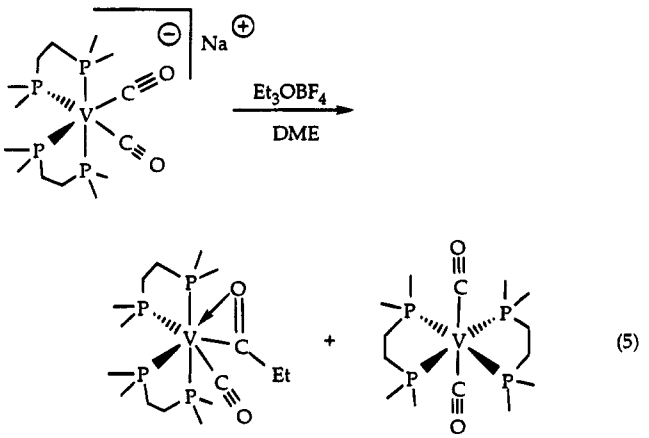

(5)

parable amounts invariably formed, one of which was readily identified as [V(CO)$_2$(dmpe)$_2$] by infrared spectroscopy and X-ray crystallography.[49] Recrystallization of the mixture from pentane at −30 °C yielded two distinct types of crystals, from which a specimen of the unidentified complex was selectively chosen. An X-ray crystal structure determination revealed incorporation of an ethyl group to provide the η^2-acyl complex [V(η^2-C(O)Et)(CO)(dmpe)$_2$] (**8**), the structure of which is depicted in Figure 2. Tables 4 and 5 provide the fractional atomic coordinates and some important distances and angles, respectively.

Although the solid-state structure resembles that of other η^2-acyl complexes,[50–52] the mechanism by which compound **8** forms is unclear. A review of the literature revealed no previous reports of direct electrophilic attack on the carbon atom of a coordinated CO ligand. Instead, a transient intermediate is typically formed, which rearranges to afford the isolated product. In the case of **8**, a vanadium alkyl species might form initially and then undergo ethyl migration to reduce steric congestion. Refluxing or photolyzing solutions of either

(48) Wells, F. J.; Wilkinson, G.; Motevalli, M.; Hursthouse, M. B. *Polyhedron* **1987**, *6*, 1351.
(49) Girolami, G. S.; Wilkinson, G.; Galas, A. M. R.; Thornton-Pett, M.; Hursthouse, M. B. *J. Chem. Soc., Dalton Trans.* **1985**, 1339.
(50) Franke, U.; Weiss, E. *J. Organomet. Chem.* **1979**, *165*, 329.
(51) Schiemann, J.; Weiss, E. *J. Organomet. Chem.* **1983**, *255*, 179.
(52) Durfee, L. D.; Rothwell, I. P. *Chem. Rev.* **1988**, *88*, 1059.

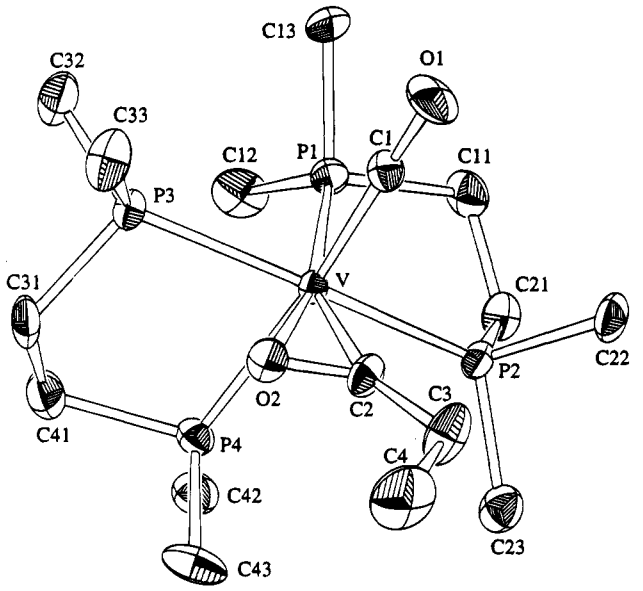

Figure 2. ORTEP diagram of [V(η^2-C(O)Et)(CO)(dmpe)$_2$] (**8**) showing 40% thermal ellipsoids for all non-hydrogen atoms.

Table 4. Positional Parameters and Equivalent Isotropic Thermal Parameters for [V(η^2-C(O)Et)(CO)(dmpe)$_2$] (8)[a]

atom	x	y	z	B(eq), Å^2 [b]
V	0.29850(9)	0.9581(1)	0.75	1.46(5)
P1	0.3028(1)	1.1428(2)	0.6883(2)	2.18(9)
P2	0.1939(1)	0.9425(2)	0.6143(2)	2.04(9)
P3	0.3865(1)	1.0155(2)	0.8933(2)	2.02(8)
P4	0.1489(1)	0.9746(2)	0.8559(2)	2.15(9)
O1	0.5023(4)	0.9206(5)	0.6481(5)	4.1(3)
O2	0.3214(4)	0.8062(4)	0.8295(4)	2.6(3)
C1	0.4239(6)	0.9369(6)	0.6876(6)	2.3(4)
C2	0.2877(6)	0.8000(6)	0.7465(7)	2.5(3)
C3	0.2742(8)	0.6906(7)	0.7034(7)	4.1(5)
C4	0.2724(9)	0.5967(7)	0.7668(9)	5.9(6)
C11	0.2504(7)	1.1488(7)	0.5681(6)	3.1(4)
C12	0.2323(7)	1.2572(6)	0.7408(7)	3.8(4)
C13	0.4286(7)	1.2077(6)	0.6687(6)	3.3(4)
C21	0.1564(7)	1.0724(7)	0.5617(6)	3.0(4)
C22	0.2532(7)	0.8761(7)	0.5126(6)	3.2(4)
C23	0.0687(7)	0.8735(7)	0.6167(6)	3.3(4)
C31	0.2989(7)	0.9934(8)	0.9928(6)	3.8(5)
C32	0.4399(7)	1.1503(7)	0.9187(6)	3.7(4)
C33	0.4957(7)	0.9337(7)	0.9284(6)	3.9(5)
C41	0.1929(7)	1.0292(9)	0.9703(6)	4.0(5)
C42	0.0349(6)	1.0593(6)	0.8383(6)	3.2(4)
C43	0.0880(7)	0.8466(7)	0.8920(7)	4.1(5)

[a] Atoms are labeled as indicated in Figure 2. Estimated standard deviations in the least significant figure are given in parentheses. [b] B(eq) = $4/3[a^2\beta_{11} + b^2\beta_{22} + c^2\beta_{33} + 2ab(\cos\gamma)\beta_{12} + 2ac(\cos\beta)\beta_{13} + 2bc(\cos\alpha)\beta_{23}]$.

[V(CO)$_2$(dmpe)$_2$Me] or [Ta(CO)$_2$(dmpe)$_2$Et], however, did not result in the formation of an acyl complex, making this possible reaction pathway unlikely. A second possibility is that an intermediate ethoxycarbyne complex forms which then undergoes a 1,2-alkyl shift to produce the acyl complex. It also is possible that the reaction proceeds through initial one-electron transfer to afford [V(CO)$_2$(dmpe)$_2$] and an ethyl radical, followed by inefficient recombination to afford the metal alkyl, the ethoxycarbyne, or the acyl complex, with the isolated species being the acyl complex. Attempts to alkylate Na[V(CO)$_2$(dmpe)$_2$] with ^{i}PrBr under a variety of conditions produced only *trans*-[V(CO)$_2$(dmpe)$_2$].

Table 5. Selected Intramolecular Bond Distances (Å) and Angles (deg) Involving the Non-Hydrogen Atoms for [V(η^2-C(O)Et)(CO)(dmpe)$_2$] (8)[a]

	Bond Distances		
V–P1	2.444(2)	V–P2	2.377(2)
V–P3	2.452(2)	V–P4	2.466(2)
V–C1	1.869(8)	V–C2	1.956(7)
V–O2	2.213(5)	C2–O2	1.27(1)
C1–O1	1.177(9)	C3–C4	1.47(1)
C2–C3	1.49(1)		
	Bond Angles		
V–C1–O1	178.1(7)	V–C2–O2	83.8(5)
C1–V–C2	84.8(3)	V–C2–C3	156.9(7)
C2–C3–C4	117.3(8)	O2–C2–C3	118.8(7)
C1–V–O2	90.7(3)	C2–V–O2	34.8(3)
P1–V–P2	77.99(8)	P1–V–P3	91.37(8)
P1–V–P4	99.41(8)	P1–V–C1	86.4(2)
P1–V–C2	157.1(3)	P1–V–O2	166.5(2)
P2–V–P4	93.70(8)	P2–V–P3	166.58(9)
P2–V–C1	95.2(3)	P2–V–C2	81.8(3)
P2–V–O2	115.4(2)	P3–V–P4	79.87(8)
P3–V–C1	92.2(2)	P3–V–C2	110.0(3)
P3–V–O2	75.6(1)	P4–V–C1	170.2(2)
P4–V–C2	92.4(3)	P4–V–O2	81.8(1)

[a] Atoms are labeled as indicated in Figure 2. Estimated standard deviations in the least significant figure are given in parentheses.

Very recently it was reported that vanadium alkyls of the form [V(CO)$_2$(dmpe)$_2$R] (R = 2,4,4-trimethyl-1-pentyl, 3-methyl-2-butyl, 3,3-dimethyl-1-butyl) can be prepared by photolyzing [V(CO)$_2$(dmpe)$_2$H] in the presence of alkenes.[53] It is not clear why the hydrovanadation of alkenes would yield vanadium alkyls whereas ethylation of [V(CO)$_2$(dmpe)$_2$]$^-$ provides an acyl complex. Obviously steric constraints cannot be the only factor that determines which species is favored, since the insertion products contain alkyls sterically more demanding than an ethyl group. From this comparison, we suggest that ethylation proceeds via initial O-alkylation of the terminal CO ligand followed by subsequent migration of the ethyl group to form the η^2-acyl species. It is also interesting to note that, as in our alkylation reactions, [V(CO)$_2$(dmpe)$_2$] forms as a byproduct in the hydrovanadation of alkenes by [V(CO)$_2$(dmpe)$_2$H].[53]

Carboxycarbyne–CO Coupling. Attempts to isolate carboxycarbyne complexes by alkylation of Na[M(CO)$_2$(dmpe)$_2$] or Na[M(CO)$_2$(depe)$_2$] (M = V, Nb, Ta) were unsuccessful. We nonetheless attempted to couple two CO ligands in these anions with carbon-based electrophiles, with the expectation that the desired intermediate M≡COR species might have sufficient lifetime to be trapped with a second equivalent of alkylating reagent to generate a stable acetylene complex. Since acetyl chloride gave excellent results in promoting siloxycarbyne–CO coupling, we focused on use of this reagent.

Treatment of a THF solution of Na[Ta(CO)$_2$(dmpe)$_2$] with acetyl chloride at room temperature gave a yellow solution, indicating formation of [Ta(CO)$_2$(dmpe)$_2$X]. Analysis of the product by IR and ^{1}H NMR spectroscopy revealed only [Ta(CO)$_2$(dmpe)$_2$Cl], and not [Ta(CO)$_2$(dmpe)$_2$Ac]. Markedly different results were obtained, however, when the reaction was run at −30 °C in DME. Rather than the yellow solution obtained at room

(53) Süssmilch, F.; Olbrich, F.; Rehder, D. *J. Organomet. Chem.* **1994**, *481*, 125.

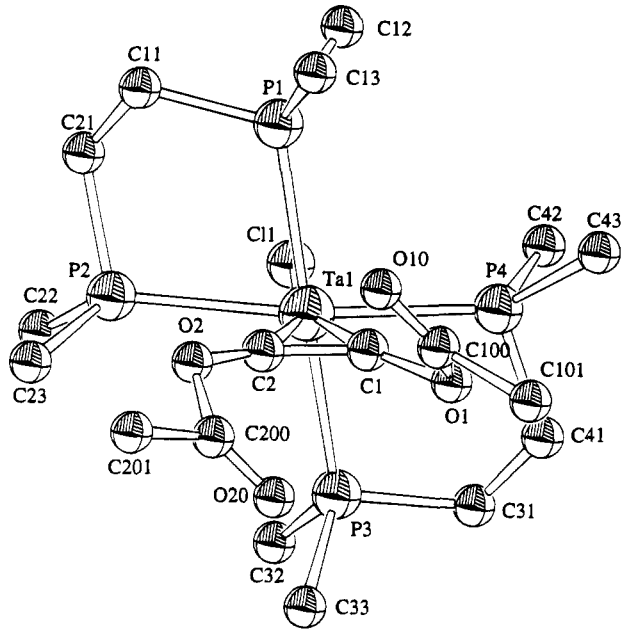

Figure 3. ORTEP diagram of [Ta(AcOC≡COAc)(dmpe)$_2$Cl] (**9**) showing 40% isotropic thermal ellipsoids for all non-hydrogen atoms.

temperature, a deep red color formed initially, which then rapidly turned green. After workup, green crystals of **9** were obtained from pentane at −30 °C. Similarly, addition of 2 equiv of acetyl chloride to a DME solution of Na[Ta(CO)$_2$(depe)$_2$] at −30 °C allowed isolation of a green crystalline product (**10**). Complexes **9** and **10** both exhibited two significant stretches in the infrared spectrum, intense bands at 1742 and 1749 cm^{-1}, respectively, attributed to the CO stretch of an acetyl group and weaker bands at 1566 and 1569 cm^{-1} for **9** and **10**, respectively, similar to values reported for the $\nu_{C\equiv C}$ stretch in previously reported disiloxyacetylene ligands. By using 2 equiv of $CH_3{}^{13}C(O)Cl$ in the syntheses of **9** and **10**, compounds **9a** and **10a** were obtained having CO stretches at 1702 and 1709 cm^{-1}, respectively, confirming the assignment of these bands. The ^{13}C NMR spectra of **9a** and **10a** have single resonances at 166.6 and 166.8 ppm, respectively. Correspondingly, their ^{1}H NMR spectra display doublets at 1.82 (J_{CH} = 6.3 Hz) and 1.83 (J_{CH} = 7.1 Hz) ppm, rather than the singlets observed for the unlabeled materials. Employing [Ta(^{13}CO)$_2$(dmpe)$_2$Cl] as the starting material afforded **9b**, which had a five-line pattern in its ^{13}C NMR spectrum centered at 200.4 ppm (J_{CP} = 14.7 Hz), in agreement with values reported for other disiloxyacetylene ligands (212.5 ppm (J_{CP} = 15 Hz) for [Ta(Me$_3$SiOC≡COSiMe$_3$)(dmpe)$_2$Cl]).[7]

Definitive structural assignment of **9** as the bis(acetoxyacetylene) complex was provided through a single-crystal X-ray analysis, an ORTEP diagram from which is presented in Figure 3. The highlight of the structure is the newly formed acetylene with two acetoxy substituents, confirming **9** as the first product of reductive coupling of two CO ligands on a group V metal promoted solely by carbon-based electrophiles. Presumably, formation of the acetylene proceeds through the acetoxy−carbyne complex [Ta(≡COAc)(CO)(dmpe)$_2$] (Scheme 4), as evidenced by the deep red solution obtained upon initial addition of acetyl chloride. This pathway is analogous to that elucidated for reductive

Scheme 4

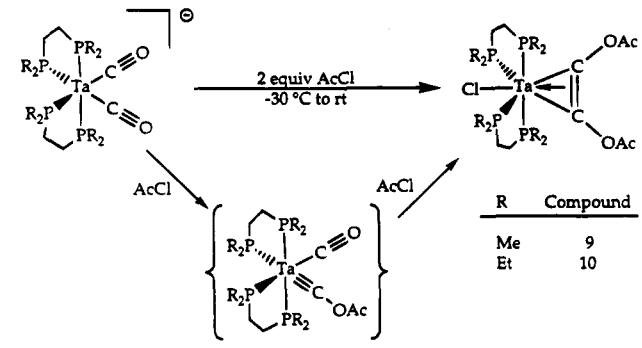

coupling with silyl reagents. Initial attempts to isolate this complex provided to be difficult, owing to its instability.

Attempts to effect coupling by treatment of Na[Ta(CO)$_2$(dmpe or depe)$_2$] with benzoyl chloride or methyl chloroformate, or by reaction of Na[Nb(CO)$_2$(dmpe)$_2$] with acetyl chloride, led instead to the corresponding dicarbonyl complexes as the major products. Efforts were also made to use carbon-based electrophiles in coupling chemistry that would result in acetylenes having a cyclic structure, analogous to cyclic coupled products of the type [M(Me$_2$SiOC≡COSiMe$_2$)(L-L)$_2$Cl] (M = V, Ta; L-L = dmpe, depe).[8] This approach was attempted to determine whether intramolecular trapping of an unstable carboxycarbyne intermediate might be faster than the corresponding intermolecular process. This strategy was unsuccessful, however, regardless of whether triphosgene, oxalyl chloride, dimethylmalonyl chloride, or succinyl chloride was employed.

Despite our inability to generalize reactions of carbon-based electrophiles for O-alkylation of the CO ligands in these complexes, the present work has established that direct O-alkylation can occur and can be used to induce new C−C bond-forming processes. Thus, earlier speculations that the formation of strong Si−O bonds is *required* to drive the silyl-based coupling process are not borne out. In this regard, it should be mentioned that proton sources react with the metal carbonyl anions [M(CO)$_2$(dmpe)$_2$]$^-$ (M = V, Nb, Ta) to afford hydrides [M(CO)$_2$(dmpe)$_2$H].[26] Hydride ligands have limited steric requirements; therefore, the formation of metal hydrides is accompanied by little or no steric barrier. Only O-silylation occurs for reactions of trialkylsilyl reagents with these complexes, consistent with the difficulty of reacting a quaternary silicon with these metal centers. On the other hand, the carbon-based electrophiles bind either at the metal center or at the carbon or oxygen atom of the CO ligand. As the size of such an electrophile increases, the likelihood of metal alkylation decreases and the formation of O-alkylated species, or complexes derived therefrom, increases. At the same time, however, the probability of electron-transfer processes increases and oxidized products of the form [M(CO)$_2$(L-L)$_2$X] or [M(CO)$_2$(L-L)$_2$] are isolated.

Summary. The reductive coupling reaction of a siloxycarbyne with an adjacent CO ligand on a group V metal has been extended to include a variety of carbon-based electrophiles. The reaction proceeded with ethyl triflate, and improved yields occurred with the bulky depe phosphine ligand. With more oxophilic reagents,

such as methyl chloroformate and acetyl chloride, high yields of coupled products were obtained, irrespective of the phosphine ligand. An X-ray crystal structure of [Ta(AcOC≡COSi^{t}BuPh$_2$)(depe)$_2$Cl] revealed the geometry about the metal center, as well as the new acetylene ligand, to be quite similar to that in the bis(siloxyacetylene) derivatives. Attempts to effect reductive coupling directly from the dicarbonyl anion with alkylating reagents normally resulted in the formation of metal alkyls or halides. One notable exception is the reaction of Na[V(CO)$_2$(dmpe)$_2$] with Et_3OBF_4, which afforded an η^2-acyl complex. In addition, under the appropriate reaction conditions, reductive coupling was achieved directly from the tantalum dicarbonyl anions Na[Ta(CO)$_2$(dmpe)$_2$] and Na[Ta(CO)$_2$(depe)$_2$] with acetyl chloride as the trapping reagent, providing the first examples of this chemistry with purely carbon-based electrophiles. In addition to extending the reductive coupling chemistry, these reactions add to the relatively scarce number of examples of direct attack of carbon-based electrophiles on carbon monoxide ligands.

Acknowledgment. This work was supported by a grant from the National Science Foundation. L.E.P. is grateful for a National Institutes of Health National Research Service Award (CA-59223).

Supplementary Material Available: Tables of bond distances and angles and anisotropic thermal parameters for **4**, **8**, and **9**, as well as structural diagrams and a table of positional parameters for **9** (21 pages). Ordering information is given on any current masthead page.

OM940981M